

Attacking Object Detectors via Imperceptible Patches on Background

Yuezun Li¹, Xian Bian² and Siwei Lyu¹

¹ University at Albany, State University of New York, NY, USA

² GE Global Research Center, Niskayuna, NY, USA

Abstract

Deep neural networks have been proven vulnerable against adversarial perturbations. Recent works succeeded to generate adversarial perturbations on either the entire image or on the target of interests to corrupt object detectors. In this paper, we investigate the vulnerability of object detectors from a new perspective — adding minimal perturbations on small background patches outside of targets to fail the detection results. Our work focuses on attacking the common component in the state-of-the-art detectors (e.g. Faster R-CNN), Region Proposal Networks (RPNs). As the receptive fields generated by RPN is often larger than the proposals themselves, we propose a novel method to generate background perturbation patches, and show that the perturbations solely outside of the targets can severely damage the performance of multiple types of detectors by simultaneously decreasing the true positives and increasing the false positives. We demonstrate the efficacy of our method on 5 different state-of-the-art object detectors on MS COCO 2014 dataset.

Introduction

Convolutional Neural Networks (CNN) have been proven vulnerable against *adversarial perturbations* (Goodfellow, Shlens, and Szegedy 2015), which are intentionally designed noises that are barely perceptible to human observers but can lead large errors on prediction results. Many works (Zeng et al. 2017; Szegedy et al. 2013; Goodfellow, Shlens, and Szegedy 2015; Kurakin, Goodfellow, and Bengio 2017; Papernot et al. 2016; Moosavi-Dezfooli, Fawzi, and Frossard 2016; Evtimov et al. 2018; Moosavi-Dezfooli et al. 2017; Luo et al. 2018; Baluja and Fischer 2018) have investigated this vulnerability and proposed various adversarial perturbation generation method to mislead image classifiers.

Recently, adversarial perturbations are extended to fail more sophisticated architectures such as object detectors, semantic and instance segmentation algorithms (Lu et al. 2017; Lu, Sibai, and Fabry 2017; Xie et al. 2017; Chen et al. 2018; Eykholt et al. 2018; Li et al. 2018). Notably, one common part of these works is that they all focused on generating adversarial perturbations either on the entire image or on the targets of interest to confuse object detectors. In

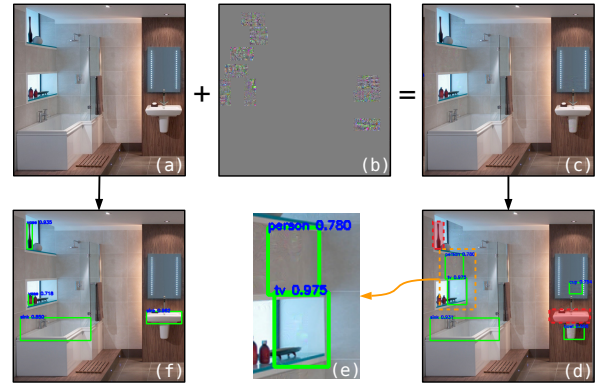


Figure 1: Visual illustration of background patches attack. (a) is original image. (b) is the background patches of adversarial perturbations we generate, which is amplified by 10 for better visualization. (c) is the perturbed image. (f, d) are detection results of (a, c) respectively. (e) is the zoomed out illustration of false positives in (d). Red boxes in (d) denote the objects that are not detected out. We can see our method not only decreases true positives, but also increases false positives.

this paper, we investigate the vulnerability of object detectors from a new perspective — we generate visually imperceptible perturbations on small background patches outside of targets, which mislead the object detectors by simultaneously decreasing the true positives and increasing the false positives. The visual illustration of background patches attack is shown in Figure 1.

Many CNN based object detectors are originated from RCNN (Girshick et al. 2014), which starts with a module generating object proposals, followed by passing each proposal to a classification CNN for class label prediction. This is further improved in the Faster-RCNN (Ren et al. 2017) structure, where the dedicated Region Proposal Networks (RPNs) is used to generate object proposals effectively. Since the convolutional nature of RPN makes its receptive field often larger than the size of proposed bounding boxes, RPNs can acquire context information outside of targets to generate accurate proposals.

However, this exactly makes them vulnerable for our background patches attacks. We target RPNs as the bottleneck of object detectors following (Li et al. 2018) as if no

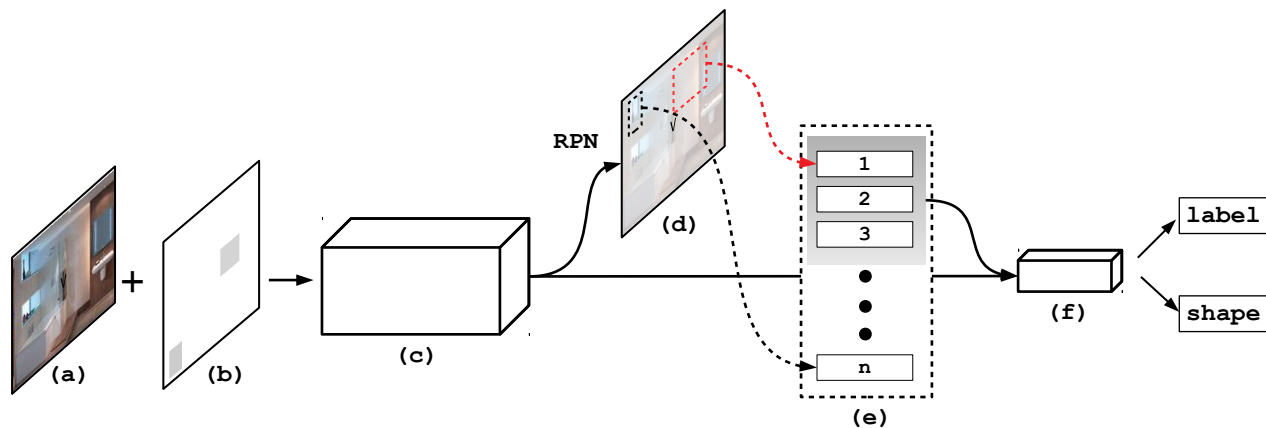


Figure 2: Overview of the goal of our imperceptible background patches attack on object detectors. (a) is the original image. (b) are the background patches adversarial perturbation. (c) is the base-network. (d) is the output proposals of Region Proposal Network (RPN). (e) is sorting process based on confidence score, where top ranked proposals are passed into (f) sub-network, which is for class label prediction and shape refinement. Red box and black box in (d) denotes false positive and true positive respectively. Our goal is to re-rank proposals such that no correct proposals can be passed into (f).

correct proposals provided, the prediction in the next stage will go wrong. RPNs usually generate a large amount of proposals. To improve the efficiency, only top ranked proposals based on confidence score are retained for final prediction. Our goal is therefore to re-rank object proposals — pushing false positive to the top and pulling true positives to the bottom. The goal of our background patches attack on object detectors is illustrated in Figure 2. To do so, we formulate background patches generation as an optimization problem of the combination of three specific loss functions — (1) *True positive confidence loss* (TPC), which aims to decrease the confidence score of true positives, *i.e.*, correct proposals, such that no correct proposal is passed into final prediction; (2) *True positive shape loss* (TPS), which aims to disturb the shape regression of correct proposals, such that even though a proposal is correctly retained by high confidence score, the shape of this proposal can still be disturbed incorrectly. Compared to shape loss proposed in (Li et al. 2018), we optimize the predicted offset automatically away from original offset instead of forcing predicted offset to a preset value; (3) *False positive confidence loss* (FPC), which aims to increase the confidence score of false positives, *i.e.*, proposals around background patches. Due to the shared feature layers with RPN and sub-networks, these false positives are very likely to be classified as one specific object category in sub-network. By optimizing overall loss function, we not only decrease true positives, but also increase false positives (see Figure 1).

Background patches attack poses server security issue in safety-critical applications, *e.g.*, a person is walking across the street with a luggage, adding adversarial perturbation on the luggage can lead detectors to fail detecting the person. A comprehensive study of this vulnerability of CNN based object detectors is therefore of importance and necessity.

We conduct experiments on MS COCO 2014 dataset (Lin et al. 2014) by attacking 5 state-of-the-art object detectors to demonstrate the efficacy of our method. Moreover, we comprehensively investigate the vulnerability with respect to key factors such as distance between background patches

and targets, object scale and distance.

Related Works

Object Detectors

Object detectors aim to localize objects in image with a class label. Current object detectors can be categorized into two classes: multi-shot and single-shot. The pipeline of multi-shot object detectors is to generate object proposals at the first step, then predict the class label and refine shape of these proposals at the second step. The classical multi-shot object detector is R-CNN (Girshick et al. 2014), which generates object proposals using selective search at first, then passes each proposal into CNN for class label prediction. Fast-RCNN (Girshick 2015) improves R-CNN using ROI layer which can make network share feature maps. Recently, Faster-RCNN (Ren et al. 2017) improves detection efficiency by using Region Proposal Networks (RPNs) to generate object proposals. RPN pre-defines a batch of anchor boxes. The proposals are generated by predicting confidence score and shape offset for each anchor box, then top ranked proposals will be selected for final prediction. RPNs are commonly used in current multi-shot object detectors. The single-shot object detectors (Redmon et al. 2016; Liu et al. 2016) are another line of research, which outputs predictions of class label and shape offset using a single pass. Thus multi-shot object detectors are more accurate and single-shot detectors are more efficient. In this paper, we only focus on investigating vulnerability of multi-shot object detectors (*e.g.*, Faster-RCNN).

Adversarial Perturbations

Adversarial perturbation is an intentionally designed and minimal perceptible noise, which can fool deep neural networks. Many methods (Evtimov et al. 2018; Szegedy et al. 2013; Goodfellow, Shlens, and Szegedy 2015; Kurakin, Goodfellow, and Bengio 2017; Papernot et al. 2016; Moosavi-Dezfooli, Fawzi, and Frossard 2016; Moosavi-Dezfooli et al. 2017; Zeng et al. 2017; Luo et al. 2018; Baluja and Fischer 2018) have been proposed to fail im-

age classifiers. The intriguing property of adversarial perturbation was first introduced by (Szegedy et al. 2013). Then an “fast gradient sign method” (FGSM) was proposed in (Goodfellow, Shlens, and Szegedy 2015) which improved the running efficiency. The “basic iterative method” was proposed in (Kurakin, Goodfellow, and Bengio 2017), which improved FGSM using iteratively adversarial perturbation generation. The work (Papernot et al. 2016) constructed an adversarial saliency map to find sensitive places that affect most. The DeepFool proposed in (Moosavi-Dezfooli, Fawzi, and Frossard 2016) simulated adversarial perturbation generation as linear classification problem, which further improved effectiveness of adversarial perturbation. The universal pattern of adversarial perturbation on specific deep neural network was proposed in (Moosavi-Dezfooli et al. 2017), which demonstrated the existence of image agnostic adversarial perturbations for image classifier.

Recently, researchers begins to explore the vulnerability of more sophisticated architectures such as object detectors. The work (Lu, Sibai, and Fabry 2017) intended to break “stop” sign and “face” detectors with adversarial perturbations on themselves. The dense adversarial generation method in (Xie et al. 2017) was proposed to iteratively break the predictions of object detectors and semantic segmentation. After that, a physical adversarial perturbation (Chen et al. 2018) is proposed to attack Faster-RCNN based “stop sign” detector. (Eykholt et al. 2018) extended this work (Chen et al. 2018) to other detectors such as YOLO, and proposed physical adversarial sticker on “stop sign” to fail detection. The work (Li et al. 2018) proposed robust adversarial perturbations which can attack Region Proposal Networks to mislead deep proposal-based models such as object detectors and instance segmentation algorithms. However, all of these methods are focused on adding adversarial perturbations on either the entire image or targets themselves. The work (Karmon, Zoran, and Goldberg 2018) generated an adversarial patch on background, but it only focused on attacking image classifiers and the adversarial perturbations had notable distortion, so that which are easily perceptible by human observers. In this paper, we investigate the vulnerability of object detectors from a new perspective — exploring the feasibility of adding invisible perturbation on small background patches to fail object detectors.

Methods

In this section, we describe our method of generating imperceptible noise added to background patches to mislead object detectors. We follows (Li et al. 2018) to target Region Proposal Networks (RPNs) as the key bottleneck of object detectors, since the RPNs are commonly used in current object detectors due to their effectiveness. We design a loss function with the combination of three terms — *True positive confidence loss* (TPC), *True positive shape loss* (TPS) and *False positive confidence loss* (FPC). The TPC aims to decrease confidence score of true positives of object proposals, such that no correct proposals can be extracted and passed into sub-network. The TPS disturbs the shape regression of true positives, therefore even proposals can be extracted correctly, their shape can also be dis-

turbed incorrectly. The FPC aims to increase the confidence score of false positives, *i.e.*, proposals around background patches. By optimizing this loss function, the proposals are re-ranked, where false positives are pushed to the top while true positives are pulled to the bottom. Since only a few top ranked proposals can be retained and passed into final prediction, our method renders the top ranked proposals to be wrong and thereby misleads the object detector. We optimize the loss function using an iterative gradient descent scheme.

Notations and Problem Formulation

Let \mathcal{I} denote the input image and $\{\bar{b}_i = (\bar{x}_i, \bar{y}_i, \bar{w}_i, \bar{h}_i)\}_{i=1}^n$ denote n ground truth bounding boxes \bar{b}_i for objects in image, where \bar{x}_i, \bar{y}_i are the x - and y -coordinate of the box center, and \bar{w}_i, \bar{h}_i are the width and height, respectively. Let \mathcal{F} denote a Region Proposal Network (RPN) with fixed model parameters. Let $\mathcal{F}(\mathcal{I}) = \{(s_j, b_j)\}_{j=1}^m$ denote the set of generated proposals on image \mathcal{I} , where s_j, b_j denotes the sigmoid confidence score and the bounding box of the j -th proposal respectively. Let $b_j = (x_j, y_j, w_j, h_j)$, where x_j, y_j are the x - and y -coordinate of the box center, and w_j, h_j are the width and height, respectively. Let $\{\mathcal{Q}_k = (\tilde{x}_k, \tilde{y}_k, \tilde{w}_k, \tilde{h}_k)\}_{k=1}^h$ denote the set of background patches added on image \mathcal{I} .

Our goal is to seek background patches with minimal distortion added that can mislead the RPN. To this end, we formulate background patches generation as an optimization problem with regards to the following loss function, which consists of three terms: TPC (L_{tpc}), TPS (L_{shape}) and FPC loss (L_{fpc}). To control the distortion of adversarial perturbation inside background patches, We employ the *Peak Signal-to-Noise Ratio* (PSNR), a widely used metric for human perception of image quality approximation. Smaller distortion leads higher value of PSNR. The background patches generation can be solved by optimizing the overall loss function with respect to background patches \mathcal{Q} on image \mathcal{I} :

$$\min_{\mathcal{I}(\mathcal{Q})} L_{tpc}(\mathcal{I}(\mathcal{Q}); \mathcal{F}) + L_{shape}(\mathcal{I}(\mathcal{Q}); \mathcal{F}) + L_{fpc}(\mathcal{I}(\mathcal{Q}); \mathcal{F}), \text{ s.t. } \text{PSNR}(\mathcal{I}(\mathcal{Q})) \geq \epsilon, \quad (1)$$

where $\mathcal{I}(\mathcal{Q})$ denotes selecting background patches \mathcal{Q} on image \mathcal{I} . $\text{PSNR}(\mathcal{I}(\mathcal{Q}))$ denotes the PSNR in area $\mathcal{I}(\mathcal{Q})$, ϵ is the lower bound of PSNR. Each loss term is described in the following.

True Positive Confidence Loss (TPC)

Similar to the previous works (Lu, Sibai, and Fabry 2017; Xie et al. 2017; Li et al. 2018) for object detection, this loss term aims to decrease the confidence score of true positives, *i.e.*, correct proposals around targets, such that no correct proposals can be extracted and passed into sub-network for final prediction. Let $z_j = 1$ denote j -th proposal is selected into TPC optimization if (1) the IoU of j -th proposal with an arbitrary ground truth bounding box is greater than a preset threshold 0.5, and (2) the confidence score of the j -th proposal is greater than a preset threshold 0.1, $z_j = 0$ otherwise. The TPC (L_{tpc}) is defined as

$$L_{tpc}(\mathcal{I}(\mathcal{Q}); \mathcal{F}) = \sum_{j=1}^m z_j \log(s_j). \quad (2)$$

Minimizing Eq. (2) decreases the confidence score of true positives.

True Positive Shape Loss (TPS)

Shape regression is an important step for proposals to refine their bounding box shape, which can adjust the shape of proposal to match the corresponding ground truth bounding boxes. Therefore attacking shape regression in RPN can also disrupt the generation of true positives, even though the confidence score of proposals is correct. Instead of forcing the predicted offset to a preset value as in (Li et al. 2018), we optimize the TPS (L_{shape}) to make predicted offset away from real offset automatically. Let $\Delta x_j, \Delta y_j, \Delta w_j, \Delta h_j$ denote the predicted x - and y - offsets of the object center, width and height offset of the bounding box b_j , respectively, $\Delta \bar{x}, \Delta \bar{y}, \Delta \bar{w}, \Delta \bar{h}$ denote the real offset between anchor boxes and ground truth bounding boxes. The TPS (L_{shape}) is defined as:

$$L_{shape}(\mathcal{I}(\mathcal{Q}); \mathcal{F}) = \exp(-\sum_{j=1}^m z_j((\Delta x_j - \Delta \bar{x})^2 + (\Delta y_j - \Delta \bar{y})^2 + (\Delta w_j - \Delta \bar{w})^2 + (\Delta h_j - \Delta \bar{h})^2)). \quad (3)$$

Minimizing Eq.(3) can gradually lead the predicted offsets $\Delta x_j, \Delta y_j, \Delta w_j, \Delta h_j$ away from $\Delta \bar{x}, \Delta \bar{y}, \Delta \bar{w}, \Delta \bar{h}$, such that the predicted shape of bounding box b_j is incorrect.

False Positive Confidence Loss (FPC)

The existing works (Lu et al. 2017; Lu, Sibai, and Fabry 2017; Xie et al. 2017; Chen et al. 2018; Eykholt et al. 2018; Li et al. 2018) only focus on decreasing true positives, we introduce an interesting loss term to increase false positives around background patches. Note that the initial proposals around background patches have low confidence score, as no objects inside background patches. Thus if we can increase the confidence score of these false positives, the ranking of proposals will be changed, *i.e.*, false positives can be pushed ahead to the top. As such, these false positives can be retained and passed into sub-network for final prediction. Due to the shared feature layers between RPN and sub-network, false positives with high confidence score can be classified as one specific object category by the sub-network. Let $r_j = 1$ denote j -th proposal is selected for FPC optimization if (1) the IoU of j -th proposal with background patches \mathcal{Q} is greater than 0.3, and (2) the IoU of j -th proposal with arbitrary ground truth bounding boxes is 0, $r_j = 0$ otherwise. The FPC (L_{fpc}) is defined as

$$L_{fpc}(\mathcal{I}(\mathcal{Q}); \mathcal{F}) = \sum_{j=1}^m r_j \log(1 - s_j). \quad (4)$$

Minimizing Eq.(4) increases the confidence score of proposals around background patches, leading to generate more false positives on background.

Background Patches Generation

Background patches adversarial perturbation should not only be effective to disturb object detectors, but also have minimal distortion visually. Thus, two factors we need to

consider when generating background patches: (1) the adversarial perturbation inside background patches, *i.e.*, $\mathcal{I}(\mathcal{Q})$ and (2) the location and size of background patches, *i.e.*, $\{\mathcal{Q}_k = (\tilde{x}_k, \tilde{y}_k, \tilde{w}_k, \tilde{h}_k)\}_{k=1}^h$. We use \mathcal{Q} in short in the following. Since optimizing the loss function with respect to these factors are difficult to get a global minimum, we employ iterative optimization scheme to alternatively solve Eq. (1) to a local minimum.

Let t denote the iteration number. We first compute the gradient of overall loss as $p_t = \nabla_{\mathcal{I}_t} \cdot (L_{tpc}(\mathcal{I}(\mathcal{Q}); \mathcal{F}) + L_{shape}(\mathcal{I}(\mathcal{Q}); \mathcal{F}) + L_{fpc}(\mathcal{I}(\mathcal{Q}); \mathcal{F}))$. Then we cluster the objects in image to several groups based on their distance of each object. We apply 3 background patches to each group.

Initializing background patches: At the first iteration, we initialize the background patches using a small size, which is 0.2 of interested target size, and get several patch shapes using different aspect ratios (1, 0.67, 0.75, 1.5, 1.33). Next we use sliding window to search the best location and shape of background patches \mathcal{Q}_t , which should satisfy: (1) intensity of gradients inside background patches $p_t(\mathcal{Q}_t)$ is maximal and (2) the distance between background patches and targets $D(\mathcal{Q}_t, \bar{b})$ should not be less than a threshold, which is defined by μ of the length of target diagonal. The above rule can be formulated as $\operatorname{argmax}_{\mathcal{Q}_t} p_t(\mathcal{Q}_t), s.t. D(\mathcal{Q}_t, \bar{b}) > \mu$. We keep the adversarial perturbations inside background patches \mathcal{Q}_t , *i.e.*, $p_t = p_t(\mathcal{Q}_t)$, which is followed by L2 normalization as $p_t = \frac{\lambda}{\|p_t\|_2} \cdot p_t$, where λ is scaling parameter. Then the image \mathcal{I} is updated and clip back to $[0, 255]$ as $\mathcal{I}_{t+1} = \operatorname{clip}(\mathcal{I}_t - p_t)$.

Expanding background patches: Next iteration, we repeat the process of adversarial perturbation p_t generation. Since we have found the initial location and shape of background patches at the first iteration, then we only expand \mathcal{Q}_t by a small stride in one of 4-directions, in terms of gradient intensity of each direction, which is followed by L2 normalization. The background patches are expanded in each iteration until the size of background patches reaches maximum value.

The iterative process is terminated until (1) maximal iteration number T is reached or (2) no correct proposals are generated around targets, *i.e.*, $\sum_{j=1}^m z_j = 0$ or (3) the RSNR($\mathcal{I}(\mathcal{Q})$) is less than a threshold ϵ . The simplified procedure of our algorithm is illustrated in Algorithm 1.

Attacking Experiments

In this section, we introduce the experiments of background patches attack in detail. We first introduce the COCO dataset we use in our experiment. Then we describes the attacking experiments on 5 state-of-the-art object detectors.

Dataset

The performance of background patches attack is evaluated on MS COCO 2014 dataset (Lin et al. 2014) under object detection track. This dataset contains 80 object class label and 1 background label. We randomly select 2000 images from MS COCO 2014 validation set for our attacking experiment. The detection performance is evaluated using ‘‘mean

Algorithm 1 background patches Generation

Require: RPN model \mathcal{F} ; input image \mathcal{I} ; maximal iteration number T .

```

1:  $\mathcal{I}_0 = \mathcal{I}, t = 0$ ;
2: while  $t < T$  and  $\sum_{j=1}^m z_j \neq 0$  do
3:    $p_t = \nabla_{\mathcal{I}_t} \cdot (L_{tpc}(\mathcal{I}(\mathcal{Q}); \mathcal{F}) + L_{shape}(\mathcal{I}(\mathcal{Q}); \mathcal{F}) + L_{fpc}(\mathcal{I}(\mathcal{Q}); \mathcal{F}))$ ;
4:   if  $t = 0$  then
5:     Initializing background patches as  $\mathcal{Q}_t$ ;
6:   else
7:     Expanding background patches as  $\mathcal{Q}_t$ ;
8:    $p_t = p_t(\mathcal{Q}_t)$ ;
9:    $p_t = \frac{\lambda}{\|p_t\|_2} \cdot p_t$ ;
10:   $\mathcal{I}_{t+1} = \text{clip}(\mathcal{I}_t - p_t)$ ;
11:  if  $\text{PSNR}(\mathcal{I}_t) < \varepsilon$  then
12:    break
13:   $t = t + 1$ ;

```

Ensure: Perturbed image \mathcal{I}_t

Table 1: Performance of background patches attack on 5 state-of-the-art object detectors at mAP 0.5 and 0.7. Lower value denotes better attacking performance.

| | FR-v16 | FR-mn | FR-rn50 | FR-rn101 | FR-rn152 |
|---------|------------------|------------------|------------------|------------------|------------------|
| Origin | 62.4/48.7 | 46.1/32.9 | 64.7/52.7 | 66.0/56.0 | 70.0/60.0 |
| Base1 | 60.8/47.9 | 41.7/29.8 | 61.6/50.6 | 62.7/53.2 | 66.3/57.1 |
| Base2 | 62.5/48.9 | 46.4/32.9 | 64.7/52.2 | 65.8/55.7 | 69.1/58.9 |
| TPC | 50.7/38.8 | 31.6/22.5 | 47.7/40.1 | 39.9/32.4 | 38.3/30.1 |
| TPS | 51.2/38.0 | 34.6/21.2 | 47.2/35.1 | 42.0/29.8 | 42.3/27.2 |
| TPC+TPS | 48.1/37.4 | 32.3/22.8 | 47.3/39.5 | 40.4/33.0 | 37.2/27.7 |
| FPC | 50.7/38.3 | 36.0/26.4 | 52.2/43.9 | 53.9/48.5 | 56.0/48.3 |
| Overall | 41.9/32.7 | 26.6/19.3 | 39.8/33.4 | 36.2/31.2 | 36.8/31.7 |

average precision” (mAP) metric (Everingham et al. 2010) at intersection-over-union (IoU) threshold 0.5 and 0.7.

Experiment Details

We conduct the proposed background patches attack experiment on Faster-RCNN object detectors based on 5 different base-networks: vgg16 (FR-v16), mobileNet (FR-mn), resnet-50 (FR-rn50), resnet-101 (FR-rn101) and resnet-152 (FR-rn152), using five cases of loss functions: (1) TPC, (2) TPS, (3) TPC+TPS, (4) FPC and (5) the summation of TPC, TPS and FPC as (Overall). We also conduct two baseline experiments to showcase the efficacy of our method. In the first experiment, we generate adversarial perturbations on the entire image using (TPC+TPS) loss, then only retain the perturbations that have at least distance μ to targets. In the second experiment, we add random noise to background patches. The random noise is under normal distribution with same distortion as our method. We denote these two baseline methods as (Base1) and (Base2)

For each case, we set maximal iteration number as $T = 250$, scale parameter as $\lambda = 30$. Typically the value of RSNR in lossy image compression is between 30 – 50 dB (Telagarapu et al. 2011). Thus we empirically set the maximal distortion as $\epsilon = 42$ dB, the distance ratio of background

Table 2: Performance of background patches attack on different object scale at mAP 0.5 and 0.7.

| | FR-v16 | FR-mn | FR-rn50 | FR-rn101 | FR-rn152 |
|---------|------------------------|------------------------|------------------------|------------------------|------------------------|
| Group 1 | 19.5/14.4 4.4/2.7 | 10.1/5.1 0.7/0.4 | 20.1/14.3 2.7/1.0 | 18.3/12.1 3.7/1.5 | 20.0/15.7 4.6/2.7 |
| Group 2 | 29.2/24.3 6.1/4.6 | 21.4/16.9 5.4/4.6 | 29.6/24.7 6.2/5.1 | 32.3/28.6 6.6/5.3 | 30.8/26.6 7.7/5.0 |
| Group 3 | 35.5/31.9 17.4/14.6 | 30.2/24.8 9.5/6.1 | 39.5/36.7 14.2/11.7 | 39.1/35.0 9.1/7.2 | 41.7/38.3 11.1/7.8 |
| Group 4 | 64.1/54.4 60.7/52.9 | 61.0/46.1 54.1/44.5 | 70.4/62.5 64.3/59.1 | 68.9/67.2 47.6/44.4 | 72.0/69.6 43.2/35.7 |

patches to target as $\mu = 0.2$.

Table 1 shows the detection performance of two baseline methods and background patches attack using five different loss functions aforementioned. Baseline method *Base1* only slightly decreases the performance of each object detector by about 3%, which demonstrates that simply using the cropped adversarial perturbations from background is not effective. Baseline method *Base2* demonstrates that the random noise added on background patches barely affect detection performance. But for our method, we can see the performance of each detector is decreased notably by at least 10% using each case of loss function. The TPC is more effective than TPS on most detectors at mAP 0.5, as TPC decreases the amount of true positives, which will affect the performance dramatically compared to only disturbing their shapes. However the TPS performs better than TPC when evaluating using mAP 0.7, as decreasing confidence score of proposals with very high confidence score to certain degree is harder than disturbing the shape of these proposals. TPC+TPS is supposed to be more effective than TPC and TPS as which considers both aspects to disturb the detection result. However, since we need to make the distortion of background patches under a maximal value, optimizing the TPC+TPS may not be faster than only optimizing TPC or TPS. Therefore, the average performance of all detectors of TPC+TPS is only a bit better than TPC and TPS at mAP 0.5. FPC leads the performance decreased about 10%, which is less compared to first three losses, as the mAP evaluation metric emphasizes the importance of false negatives. However, in practice use, false positives are also critical for security issue. Due to simultaneously decreasing true positives and increasing false positives, the Overall loss shows best performance compared to other losses, which decreases the performance by at least 20% at both mAP 0.5 and mAP 0.7 for all detectors.

Figure 5 illustrates several examples of using losses TPC+TPS, FPC and Overall. For example, the glass bottle (denote by red box) in (FR-mn, TPC+TPS) is missed out as the TPC+TPS loss term decreasing true positives and several false positives are generated around background patches in (FR-mn, FPC) as FPC loss term increasing false positives. Since the Overall loss considers both, *i.e.*, decreasing true positives and increasing false positives, the detection result of (FR-mn, Overall) not only fails to detect the glass bottle, but also raise many false positives.

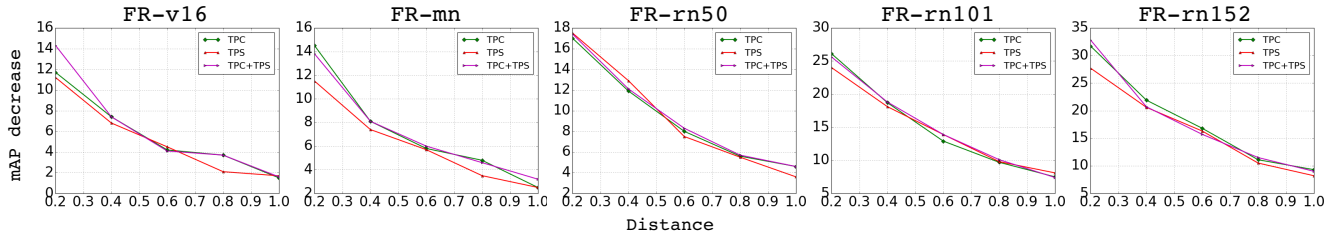


Figure 3: Performance of background patches attacks at mAP 0.5 on 5 object detectors as the distance between background patches and targets increases. We do not consider FPC, since it has no relation with the distance between background patches and targets.

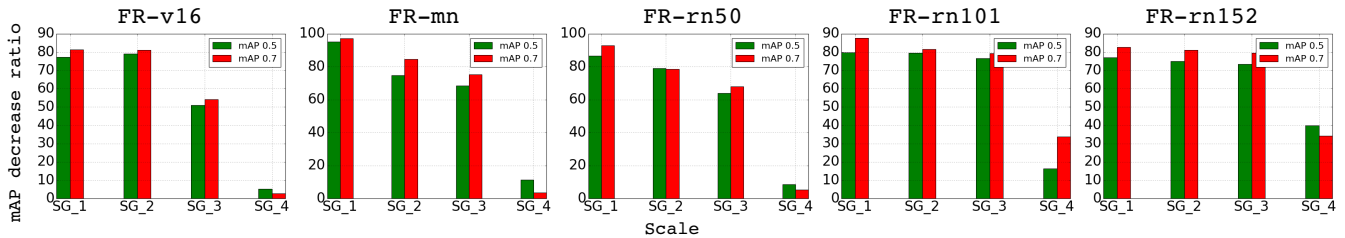


Figure 4: Performance of background patches attacks at mAP 0.5 and 0.7 on different object scales on 5 object detectors. SG_1 - SG_4 denote the 4 object groups sorted based on their size by ascending order.

Ablation Study

In this section, we comprehensively investigate the vulnerability of object detectors with respect to the distance between background patches and targets, object scale and distance.

Distance between background patches and targets

Due to the convolutional nature in RPNs, the receptive field of each proposal is much larger than itself. Thus the prediction result can be disturbed by only adding adversarial perturbation patches outside targets. In this section, we investigate whether background patches have same effect at arbitrary location inside its theoretically receptive field. We conduct experiments to show attacking performance with various distance between background patches and targets. We use the decrease of detection performance to denote the attacking performance. Since FPC has no relation with the distance between background patches and targets, we only consider three loss cases (TPC, TPS and TPC+TPS) that decreasing true positives. Figure 3 illustrates the attacking performance as the distance between background patches and targets increases. We observe that attacking performance decreases as the distance increases, which indicates despite the receptive field is theoretically very large, the effectiveness of background patches attack gradually decreases as the distance increases, which is consistent with the explanation of receptive field in CNN (Zhou et al. 2014). We illustrate the detection result of FR-rn152 in Figure 6, which is attacked by background patches as the distance increases. We can see the left person in image is gradually detected out correctly as the distance increases.

Object Scale

We investigate that whether object scale can affect background patches attack performance on object detectors. We cluster objects of dataset into 4 groups according to their

size, and sort the group by ascending order. Then we conduct experiments on each group to compare attacking performance. Table 2 shows the detection performance before and after background patches attack on different object scale. The first row in a group denotes the original detection performance, the second row denotes the detection performance after background patches attack. For better visualization, we plot the performance decrease ratio in Figure 2, where the SG_1 - SG_4 denote the 4 object groups sorted based on their size by ascending order, y-axis is the detection performance decrease ratio. We observe that small objects are easier to be disturbed than large objects, under the same perturbation amount, which is controlled by the maximum distortion on patches and the size of patches. This may be due to the fact that the convolution kernel size is fixed in each layer, so that the ratio of context in surrounding background to small object is larger than large object, *i.e.*, more ratio of surrounding context can be seen when to detect small object. As shown in (FR-rn50, TPC+TPS) of Figure 5, the detection of dog at the right-bottom corner is missed while the television is still successfully detected.

Discussion

We observe a direct relation between the number of patches and the object distance distribution. In particular, the smaller distances among objects, the fewer background patches needed to successfully disturb the output. In the experiments, we normalize the mean object distance to $[0, 1]$ by dividing the minimal dimension of image and we categorize all test images into 5 groups with different mean object distance and find out the mean number of background patches needed per object. As shown in Figure 7, the number of patches per object reduces as the mean distance between objects in one image decreases. DG_1 - DG_5 denote the 5 groups which have mean object distance, 0.55, 0.30, 0.23, 0.18, 0.09, respectively. It is also caused by

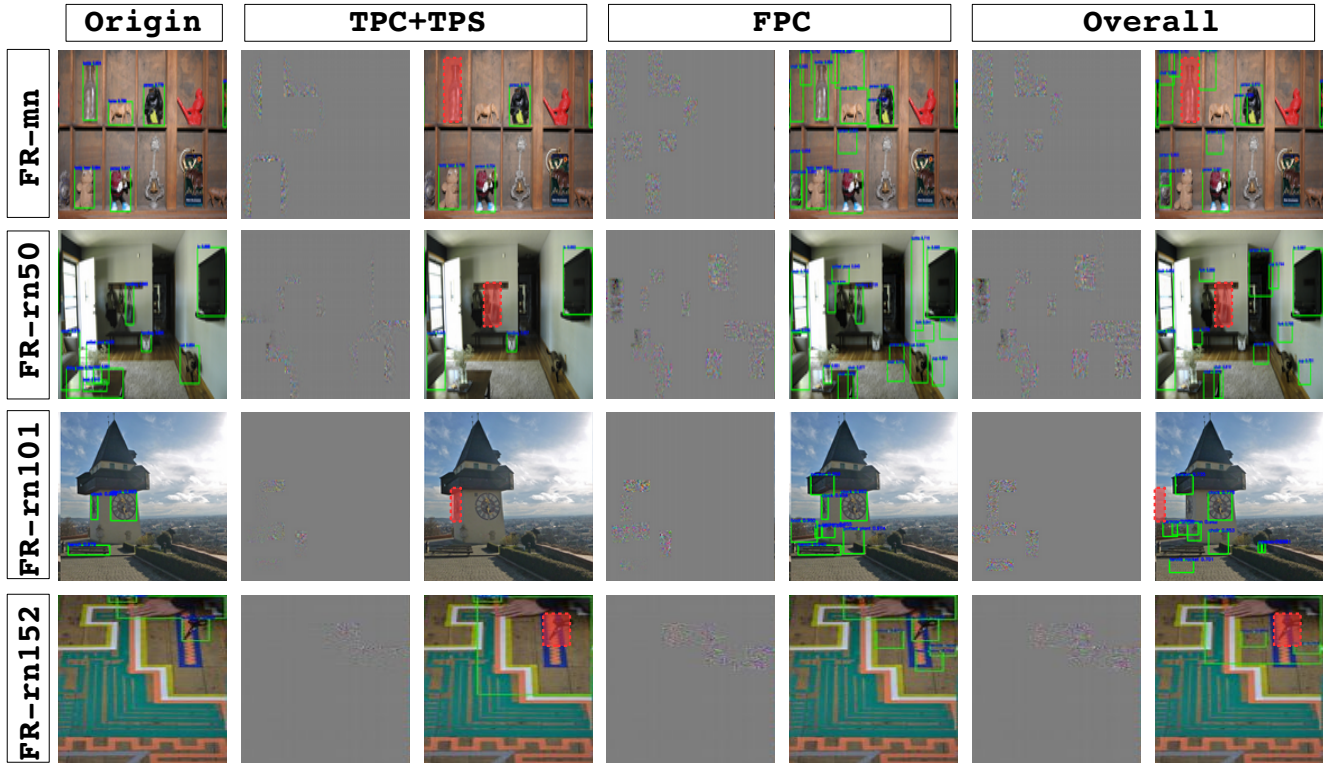


Figure 5: Visual illustration of background patches attacks on 4 object detectors using different loss. Each column includes the visualization of background patches perturbation and disturbed detection results. We can see that several true positives are missed out (highlighted by red box) in TPC+TPS column and false positives are generated in FPC column. Using overall loss not only decreases true positives, but also increases false positives, shown in Overall column.

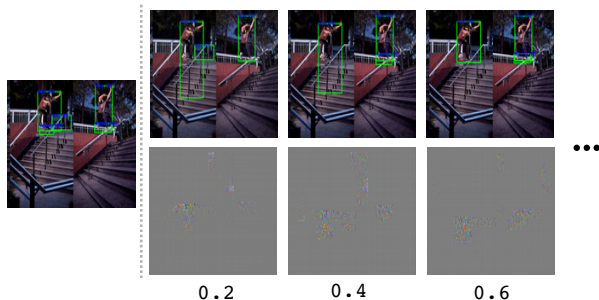


Figure 6: The left image is the original detection result on FR-rn152. The right part is the illustration of detection result attacked by background patches as the distance between background patches and targets increases. We can see the detector gradually detect the person on the left side of image as the distance increases.

the effect of receptive field. Specifically, when the objects are close to each other, their receptive fields also overlap, which implies that one patch can impact the detection of more than one object.

Conclusion

In this paper, we investigate the vulnerability of object detectors by adding minimal perturbations on small background patches outside of targets to degrade the detection performance. Our work targets the Region Proposal Network as

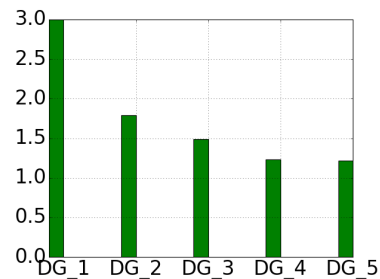


Figure 7: Illustration of the number of patches per object as the mean distance between objects in one image decreases. DG_1 - DG_5 denote the 5 groups which have mean object distance, 0.55, 0.30, 0.23, 0.18, 0.09, respectively.

the key bottleneck of object detectors due to their commonly usage in the state-of-the-art detectors (e.g. Faster R-CNN). To do so, we propose a novel method to generate background perturbation patches, to damage the performance of multiple types of detectors by simultaneously decreasing the true positives and increasing the false positives. Our experiments are conducted on MS COCO 2014 dataset of attacking on 5 different state-of-the-art object detectors to demonstrate the efficacy of our method. The future work includes to improve the optimization process of our method and attempt to analyze the scene robustness under image space.

References

- [Baluja and Fischer 2018] Baluja, S., and Fischer, I. 2018. Learning to attack: Adversarial transformation networks. In *AAAI*.
- [Chen et al. 2018] Chen, S.-T.; Cornelius, C.; Martin, J.; and Chau, D. H. 2018. Robust physical adversarial attack on faster r-cnn object detector. *arXiv preprint arXiv:1804.05810*.
- [Everingham et al. 2010] Everingham, M.; Van Gool, L.; Williams, C. K.; Winn, J.; and Zisserman, A. 2010. The PASCAL visual object classes (VOC) challenge. *IJCV*.
- [Evtimov et al. 2018] Evtimov, I.; Eykholt, K.; Fernandes, E.; Kohno, T.; Li, B.; Prakash, A.; Rahmati, A.; and Song, D. 2018. Robust physical-world attacks on deep learning models. In *CVPR*.
- [Eykholt et al. 2018] Eykholt, K.; Evtimov, I.; Fernandes, E.; Li, B.; Rahmati, A.; Tramer, F.; Prakash, A.; Kohno, T.; and Song, D. 2018. Physical adversarial examples for object detectors. *arXiv preprint arXiv:1807.07769*.
- [Girshick et al. 2014] Girshick, R.; Donahue, J.; Darrell, T.; and Malik, J. 2014. Rich feature hierarchies for accurate object detection and semantic segmentation. In *CVPR*.
- [Girshick 2015] Girshick, R. 2015. Fast R-CNN. In *ICCV*.
- [Goodfellow, Shlens, and Szegedy 2015] Goodfellow, I. J.; Shlens, J.; and Szegedy, C. 2015. Explaining and harnessing adversarial examples. In *ICLR*.
- [Karmon, Zoran, and Goldberg 2018] Karmon, D.; Zoran, D.; and Goldberg, Y. 2018. Lavan: Localized and visible adversarial noise. *arXiv preprint arXiv:1801.02608*.
- [Kurakin, Goodfellow, and Bengio 2017] Kurakin, A.; Goodfellow, I.; and Bengio, S. 2017. Adversarial examples in the physical world. In *ICLR*.
- [Li et al. 2018] Li, Y.; Tian, D.; Chang, M.; Bian, X.; and Lyu, S. 2018. Robust adversarial perturbation on deep proposal-based models. In *BMVC*.
- [Lin et al. 2014] Lin, T.-Y.; Maire, M.; Belongie, S. J.; Hays, J.; Perona, P.; Ramanan, D.; Dollár, P.; and Zitnick, C. L. 2014. Microsoft COCO: Common objects in context. In *ECCV*.
- [Liu et al. 2016] Liu, W.; Anguelov, D.; Erhan, D.; Szegedy, C.; Reed, S.; Fu, C.-Y.; and Berg, A. C. 2016. Ssd: Single shot multibox detector. In *ECCV*, 21–37. Springer.
- [Lu et al. 2017] Lu, J.; Sibai, H.; Fabry, E.; and Forsyth, D. 2017. Standard detectors aren't (currently) fooled by physical adversarial stop signs. *arXiv preprint arXiv:1710.03337*.
- [Lu, Sibai, and Fabry 2017] Lu, J.; Sibai, H.; and Fabry, E. 2017. Adversarial examples that fool detectors. *arXiv 1712.02494*.
- [Luo et al. 2018] Luo, B.; Liu, Y.; Wei, L.; and Xu, Q. 2018. Towards imperceptible and robust adversarial example attacks against neural networks. In *AAAI*.
- [Moosavi-Dezfooli et al. 2017] Moosavi-Dezfooli, S.-M.; Fawzi, A.; Fawzi, O.; and Frossard, P. 2017. Universal adversarial perturbations. In *CVPR*.
- [Moosavi-Dezfooli, Fawzi, and Frossard 2016] Moosavi-Dezfooli, S.-M.; Fawzi, A.; and Frossard, P. 2016. Deepfool: a simple and accurate method to fool deep neural networks. In *CVPR*.
- [Papernot et al. 2016] Papernot, N.; McDaniel, P.; Jha, S.; Fredrikson, M.; Celik, Z. B.; and Swami, A. 2016. The limitations of deep learning in adversarial settings. In *EuroS&P*.
- [Redmon et al. 2016] Redmon, J.; Divvala, S.; Girshick, R.; and Farhadi, A. 2016. You only look once: Unified, real-time object detection. In *CVPR*, 779–788.
- [Ren et al. 2017] Ren, S.; He, K.; Girshick, R.; and Sun, J. 2017. Faster R-CNN: Towards real-time object detection with region proposal networks. *TPAMI*.
- [Szegedy et al. 2013] Szegedy, C.; Zaremba, W.; Sutskever, I.; Bruna, J.; Erhan, D.; Goodfellow, I.; and Fergus, R. 2013. Intriguing properties of neural networks. *arXiv 1312.6199*.
- [Telagarapu et al. 2011] Telagarapu, P.; Naveen, V. J.; Prasanthi, A. L.; and Santhi, G. V. 2011. Image compression using DCT and wavelet transformations. *International Journal of Signal Processing, Image Processing and Pattern Recognition*.
- [Xie et al. 2017] Xie, C.; Wang, J.; Zhang, Z.; Zhou, Y.; Xie, L.; and Yuille, A. 2017. Adversarial examples for semantic segmentation and object detection. In *ICCV*.
- [Zeng et al. 2017] Zeng, X.; Liu, C.; Qiu, W.; Xie, L.; Tai, Y.-W.; Tang, C. K.; and Yuille, A. L. 2017. Adversarial attacks beyond the image space. *arXiv 1711.07183*.
- [Zhou et al. 2014] Zhou, B.; Khosla, A.; Lapedriza, A.; Oliva, A.; and Torralba, A. 2014. Object detectors emerge in deep scene cnns. *arXiv preprint arXiv:1412.6856*.